Polymer 143 (2018) 155–163

Contents lists available at ScienceDirect

Polymer

journal homepage: www.elsevier.com/locate/polymer

Waterborne acrylic resin modified with glycidyl methacrylate (GMA): Formula optimization and property analysis

Xingkui Guo [a], Shengsong Ge [a, *], Junxiang Wang [a], Xincheng Zhang [a], Tao Zhang [a], Jing Lin [b, **], Cindy Xinxin Zhao [c], Bin Wang [d, ***], Guangfei Zhu [a], Zhanhu Guo [c, ****]

[a] College of Chemical and Environmental Engineering, Shandong University of Science and Technology, Qingdao, 266590, China
[b] School of Chemistry and Chemical Engineering, Guangzhou University, Guangzhou, 510006, China
[c] Integrated Composites Laboratory (ILC), Department of Chemical & Biomolecular Engineering, University of Tennessee, Knoxville, TN 37996, USA
[d] Engineered Multifunctional Composites (EMC) Nanotechnology LLC, Knoxville, TN 37934, USA

ARTICLE INFO

Article history:
Received 21 January 2018
Received in revised form
25 March 2018
Accepted 3 April 2018
Available online 5 April 2018

Keywords:
Glycidyl methacrylate
Silane coupling agent
Waterborne acrylic resin
Anticorrosion

ABSTRACT

Novel waterborne acrylic resin modified with glycidyl methacrylate (GMA) was successfully synthesized via homogeneous solution polymerization in isopropyl alcohol followed by solvent exchange with water. Aminopropyltriethoxysilane (KH-550), a silane coupling agent that can crosslink with resin and iron base material, was used as curing agent for solidifying this GMA modified resin. The cured mechanism of the coating was also investigated by ^{29}Si nuclear magnetic resonance (^{29}Si NMR) spectra and attenuated total reflectance-Fourier transform infrared spectroscopy (ATR-FTIR). The waterborne acrylic resin was sprayed on the iron base material and cured by KH-550 for 30 min at 100 °C to form the desired coating. The GMA and KH-550 were found to significantly decrease the curing temperature of this two-component waterborne resin. The thermal property of the coatings with different GMA loadings was investigated using differential scanning calorimetry (DSC) and thermogravimetric analysis (TGA). The GMA enhanced the thermal stability of the coatings from 100 to 400 °C. The modification of GMA was found to reinforce significantly the mechanical properties of the coatings. The tensile strength of coating modified with 15 wt% GMA got a 78.65% improvement compared to that of unmodified resin. The surface hydrophobicity of the coatings does get affected by this modification. The contact angle got increased from 87.72°of the unmodified resin coating to 99.51°of coating modified with 15 wt% GMA. This work opens a new way to synthesize high performance waterborne acrylic resin and reports on the anti-flash corrosion of waterborne coatings on the iron base material surface.

1. Introduction

Nowadays, due to the imposition of legislative restrictions on the utilization and emission of volatile organic compounds (VOC) [1,2], waterborne coatings find increasing importance among the multifarious high performance solvent-borne coatings [3,4]. Meanwhile, with a series of potential benefits (e.g., non-toxic, non-flammable, environmental friendly, low energy curing concern) [5,6], which are not exhibited by solvent-based paints and coating, waterborne coatings have received tremendous attention for ambient curing coating applications [7–12]. However, the conventional waterborne coating finishing agent with the extensive use of surfactants limits good properties of the finishing materials and causes the pollution to the environment [13,14]. As a result, remarkable properties of emulsifier-free waterborne resin have attracted wide attention from many scientific and practical viewpoints as the finishing materials [15].

One-component waterborne acrylic resin has grown commercially over the last forty years [16]. Although it has many good properties such as user-friendly [17,18], one-component waterborne acrylic resin, belonging to thermoplastic systems, has some deficiencies (e.g., insufficient hydrolytic stability, lower water resistance, poor chemical resistance) [19–22]. Moreover, the dichotomy between lower VOC content and strong hardness is another example which is actively being pursued in the coating

* Corresponding author.
** Corresponding author.
*** Corresponding author.
**** Corresponding author.
E-mail addresses: geshs@163.com (S. Ge), linjing@gzhu.edu.cn (J. Lin), bwang409@yahoo.com (B. Wang), zguo10@utk.edu (Z. Guo).

https://doi.org/10.1016/j.polymer.2018.04.020
0032-3861/

markets, and is also a particularly challenging target for one-component waterborne acrylic coatings at the same time [23–25]. High levels of pre-crosslinking can not be easily introduced into one-component waterborne acrylic resin because of high viscosity of prepolymers or poor coalescence of the formulated dispersions [26,27].

Two-component waterborne coating materials have attracted great interests in both academic and industrial fields because of the increasingly strict requirements for high performance coatings. As we know, the type and dosage of the curing agent for two-component waterborne acrylic resin affect the performance of the final coating [28,29]. Furthermore, because water is the only solvent used in the water-based acrylic resin system, the curing agent must be water-soluble or water dispersible. The active functional groups in the curing agent need be selected based on the type of active functional groups in the water-based resin. The compatibility of these two is also an important parameter affecting the curing process [30]. The presence of the curing agent can also improve the cross-linking density [31]. Chemical reactions between different polar groups not only facilitate cross-links and thus enhance the physical and chemical integrity of the coalesced film [32–34], but also reduce the number of polar groups and thereby lower the water sensitivity of the coatings [35]. Among the common curing agents, various isocyanates are most popular in the two-component waterborne acrylic resin [36,37], because isocyanates can improve the properties (e.g., mechanical, wear, chemical resistance, outdoor durability and adhesive properties) of the coatings through reacting with the waterborne acrylic resin [38–40]. However, they have some deficiencies such as side reaction, high cost and toxicity and can not avoid flash corrosion [41] (In the film form process of waterborne coating, the metal surface oxidizes and forms rust spots during a very short period of time) of the iron base materials [42]. The quest to develop new curing agent has been the subject of a great deal of activities in recent years [43]. Thus, to fabricate green and high performance coatings with a simple, low-cost, continuous and scalable approach is still a big challenge for next generation coatings industry.

In this study, two-component waterborne acrylic resin modified with glycidyl methacrylate (GMA) was designed and synthesized successfully by homogeneous solution polymerization in isopropyl alcohol. Aminopropyltriethoxysilane (KH-550) was used as coupling agent that not only crosslinked with resin and iron based material but also introduced Si-O-Si and Si-O-C in the coating to enhance the performance of the coating (e.g., good adhesion and improve the water resistance). The KH-550 as curing agent was the first attempt in the two-component waterborne acrylic resin system. The cured mechanism of the coating was also investigated by ^{29}Si nuclear magnetic resonance (^{29}Si NMR) spectra and attenuated total reflectance-Fourier transform infrared spectroscopy (ATR-FTIR). The thermal property of the coatings was investigated using differential scanning calorimetry (DSC) and thermogravimetric analysis (TGA). The mechanical property of the coatings was investigated via tensile test and the fracture mechanism was disclosed by scanning electron microscope (SEM) observations. The surface wettability of the coatings was investigated by measuring water contact angle with the sessile drop method. The thermal and mechanical properties of these two-component waterborne resin were affected by GMA (e.g., decreased curing temperature, improved crosslinking density, strengthened mechanical property). In addition, anti flash corrosion was observed for the film coating by these novel waterborne acrylic resin and curing agent.

2. Experimental

2.1. Materials

Methyl methacrylate (MMA, Analytical Reagent), butyl acrylate (BA, Analytical Reagent), acrylic acid (AA, Analytical Reagent), 2-ethylhexyl acrylate (2-EHA, Analytical Reagent), isopropyl alcohol (IPA, Analytical Reagent), glycidyl methacrylate (GMA, Analytical Reagent), hydroxyethyl methacrylate (HEMA, Analytical Reagent), N,N - dimethyl ethanolamine (DMEA, Analytical Reagent), maleic anhydride (MAH, Analytical Reagent), and 2,2-azobisisobutyronitrile (AIBN, Analytical Reagent) were obtained from Tianjin BASF Chemical Co. While aminopropyltriethoxysilane (KH-550, Analytical Reagent) was purchased from Tianjin Commio Chemical Reagent Company. All the materials were used as-received without any further purification or analysis.

2.2. Synthesis of waterborne acrylic resin

Different acrylic monomers play different roles in the polymer chains. The function of monomer in the formula are as follows. The methyl methacrylate is a hard monomer that can enhance the hardness and gloss of waterborne resin. The butyl acrylate is a soft monomer that can enhance the chain flexibility of waterborne resin. The 2-ethylhexyl acrylate can provide the plasticity of waterborne resin. The acrylic acid, maleic anhydride and hydroxyethyl methacrylate, are functional monomers and can provide polar functional groups such as carboxyl and hydroxy, allowing acrylic polymers to dissolve in water. Meanwhile, the polar functional groups can react with curing agent in the curing process.

A 250 mL round-bottomed, four-necked flask equipped with a mechanical stirrer, condenser, and thermometer was used as a reactor vessel for the polymerization reaction. The polymerization was carried out in a constant temperature water bath. Firstly, 13.4 g MMA, 19.6 g BA, 2.7 g MAH, 3.3 g 2-EHA, 3.3 g AA, 4.1 g HEMA, and 0.9 g AIBN were mixed in the beaker at room temperature to form a clear solution (mixture A). 2.4 g HEMA, 8.3 g IPA, and 0.3 g AIBN were mixed in another beaker at room temperature to form a clear solution (mixture B). Secondly, the mixture A was added dropwise to the reactor with 41.7 g IPA at 82 °C for 30 min. After adding all mixture A, the reaction was continued for another 30 min at 82 °C. Thirdly, the reactor was heated up to 85 °C, and mixture B was added dropwise to the reactor at 85 °C within 20 min. After all mixture B was added, the reaction was continued for another 3 h at 85 °C (Table 1). Subsequently, the as-synthesized product (99.5 g) was cooled down to room temperature,and 4.3 g DMEA was added under continuous stirring for 20 min to neutralize the free carboxylic acid groups in the resin chains. Finally, 42.9 g water was added dropwise over 40 min at agitation speed of 550 rpm to prepare stable waterborne resin with 35 wt% solid contents.

2.3. Modification of waterborne acrylic resin (WA/GMA)

The waterborne acrylic resin modified with glycidyl methacrylate (GMA) was synthesized following the same procedures as descried in section 2.2. The only difference was that mixture A and mixture B were added with different GMA loadings, namely WA/GMA0 (0 wt% GMA of the total monomers), WA/GMA5 (5 wt% GMA of the total monomers), WA/GMA15 (15 wt% GMA of the total monomers) and WA/GMA30 (30 wt% GMA of the total monomers).

Table 1
The ingredient of the waterborne acrylic resin.

Monomer (g)						Initiator (g)	Solvent (g)	Total (g)
MMA	BA	MAH	2-EHA	AA	HEMA	AIBN	IPA	100
13.4	19.6	2.7	3.3	3.3	6.5	1.2	50	

1/3 of the GMA was added to the mixture A and the 2/3 of the GMA was added to the mixture B.

2.4. Film preparation

Different weights of waterborne resin and curing agent (the curing agent was diluted with water at a mass ratio of 1:2) were mixed at room temperature. The mixture was magnetically stirred for 2–6 min depending on curing agent concentration, i.e., longer time for higher concentrations. Then the mixture was sprayed by an airbrush (W-71, Anest Iwata) at a gas flow rate of 150 L/min, and a movement speed of 30–40 cm/s on the tinplate substrates and dried at room temperature for 24 h until the mixture was not able to flow on the tinplate substrates. The coated substrates were transferred to an oven and cured for 30 min at 100 °C. The waterborne resin unmodified with GMA was prepared using the same processing protocol for comparison. The hydroxyl group of silicane tends to react with the hydroxyl group on the surface of the tinplate to form the molecular layer of silicane. The molecular layer of silicane acts as a bridge between coating and tinplate. The curing process is schematically shown in Scheme 1.

The mass ratio of WA/GMA to KH-550 was important for the mechanical properties and surface performance of the coatings. WA and GMA could not react completely when KH-550 was not enough. Therefore, the WA/GMA-KH-550s were prepared with different mass ratios of WA/GMA and KH-550 to evaluate the influence of mass ratio on the mechanical and surface performance of WA/GMA-KH-550. These samples were marked as WA/GMA-KH-550 (m:n) to designate the samples prepared with the mass ratio (m:n) of WA/GMA and KH-550.

2.5. Characterizations

The attenuated total reflectance-Fourier transform infrared spectroscopy (ATR-FTIR, Nicolet 380, Thermo Fisher Scientific Co., USA) was used to determine the chemical structure of waterborne resin and coatings.

High-resolution ^{29}Si-NMR spectra were obtained at a frequency of 79.45 MHz (9.4 T) with a Varian Unity INOVA spectrometer. The measurements were carried out under Magic Angle Sample Spinning (MAS) up to 5 kHz in zirconia rotors with a Varian 7 mm wide-body probe. The spectra were obtained from Bloch Decay (BD) signals after p/2 pulses of 4 ms length with 30 s recycle time by collecting up to 3000 free induction decay (FID) signals.

The curing temperature was determined by differential scanning calorimeter (DSC, DSC1, Mettler Toledo Co. Swiss Confederation). The uncured samples (about 10 mg) were heated from 25 to 150 °C under a nitrogen atmosphere at a nitrogen flow of 20 mL/min. The thermal stability of the cured samples was characterized by using a thermogravimetric analyzer (TGA, Mettler Toledo Co. Swiss Confederation). About 10 mg mixture of the curing agent and the waterborne resin at different rations was introduced into the thermobalance, and then heated from 25 to 800 °C at a heating rate of 15 °C/min and a nitrogen flow of 20 mL/min.

The tensile experiments were carried out on a tensile tester (WDW3100, Changchun Kexin Co., China) at a cross-head speed of 2 mm/min at room temperature following ASTM-D638. The dimensions of the tensile specimens were 10 mm × 4 mm in the

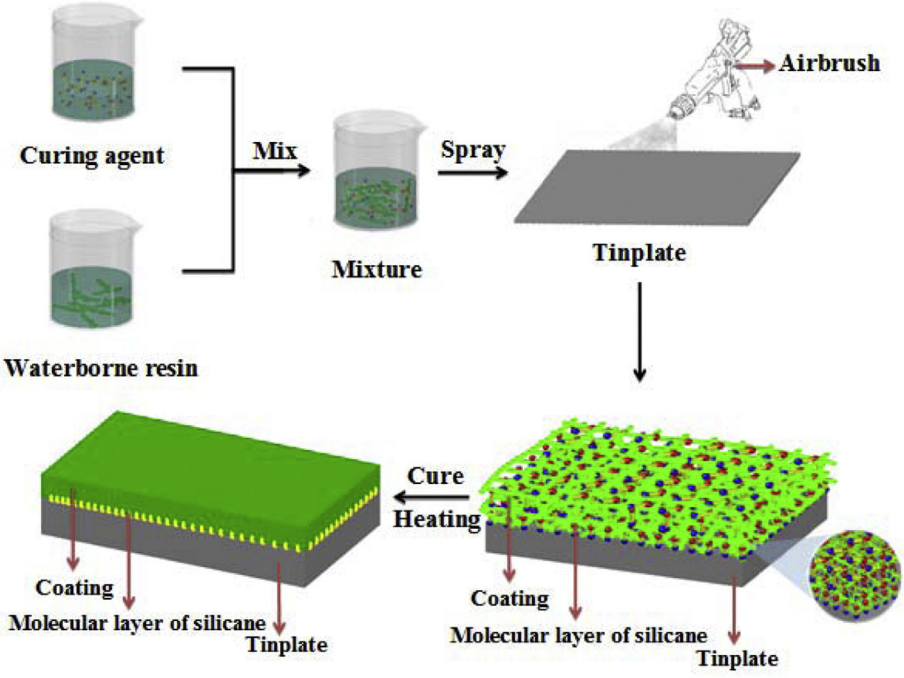

Scheme 1. Schematic representation of curing process.

working section. At least three specimens of each sample were tested. After the tensile test, the broken samples were collected, and the morphology and elemental analysis of the fracture surfaces were characterized by a field emission scanning electron microscope (SEM, SU-70, Hitachi, Japan) at an acceleration voltage of 30 kV.

The contact angles of the coatings were measured on a DSA30 machine (Data-Physics, Germany) at ambient temperature. The water droplets (about 5 μL) were dropped carefully onto the surface of materials. The average value of five measurements performed at different positions on the same sample was adopted as the contact angle.

3. Results and discussion

3.1. Curing behavior

The performance of final film was influenced by the curing extent. In the curing process of the two-component waterborne acrylic resin, the reaction between acrylic chain and curing agent is critical for the quality of the final coating. In the WA/GMA-KH-550 systems, the following reactions may occur during the curing process as shown in Scheme 2. Dehydration reaction will occur between KH-550 molecular (Scheme 2a). The hydroxyl groups in the waterborne acrylic chains will react with the amino and hydroxyl groups in the KH-550 (Scheme 2b). The carboxyl groups in the waterborne acrylic chains will react with the hydroxyl groups in the KH-550 (Scheme 2c). The hydroxyl groups on the metal surface will react with the hydroxyl groups in the KH-550 and acrylic chains (Scheme 2d and 2e).

Fig. 1 shows the FTIR spectra of WA/GMA15 and WA/GMA15-KH-550 (1:0.15) at different curing time. The peaks at 3375, 1732, 1303 and 1139 cm^{-1} correspond to the stretching absorption of the −OH, C═O, C-N and C-O-C, respectively [44–48]. The peak at 1209 cm^{-1} represents the stretching resonance of C-O of the carboxylic acid [48,49]. The weak absorption peaks at 1066 and 825 cm^{-1} belong to the extending vibration of the Si-O-Si and Si-O-C groups, respectively [50–52].

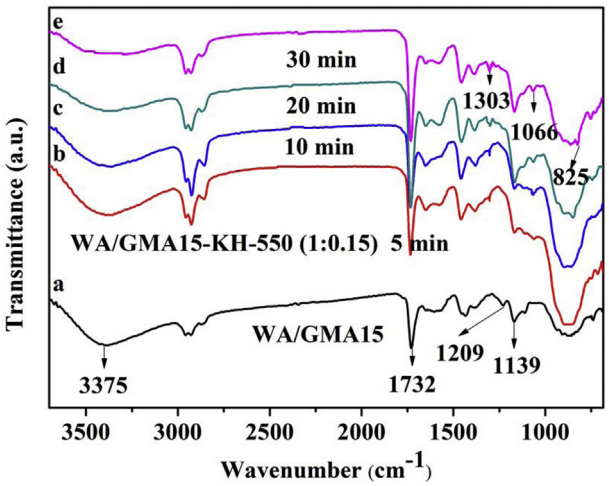

Fig. 1. FTIR spectra of (a) WA/GMA15; and WA/GMA15-KH-550 (1:0.15) prepared with a curing time of (b) 5, (c) 10, (d) 20, (e) 30 min.

In comparison with pure resin, the characteristic absorption bands at 3375 and 1229 cm^{-1} respectively assigned to the stretching resonances of −OH and -COOH are weakened, illustrating that partial hydroxyl groups (Scheme 2b) and carboxylic acid (Scheme 2c) have reacted with the hydroxyl groups of KH-550. At the same time, the new weakened peaks appeared at 825, 1066, and 1303 cm^{-1}. These characteristic peaks also indicate that KH-550 has reacted with the hydroxyl groups in the chain of waterborne resin (Scheme 2b) and dehydration reaction occurred (Scheme 2a). The results indicate that two component waterborne coating has been cured upon heating.

The conversion of the hydrolyzed KH-550 to the silica network was measured with solid-state ^{29}Si NMR analysis, as shown in

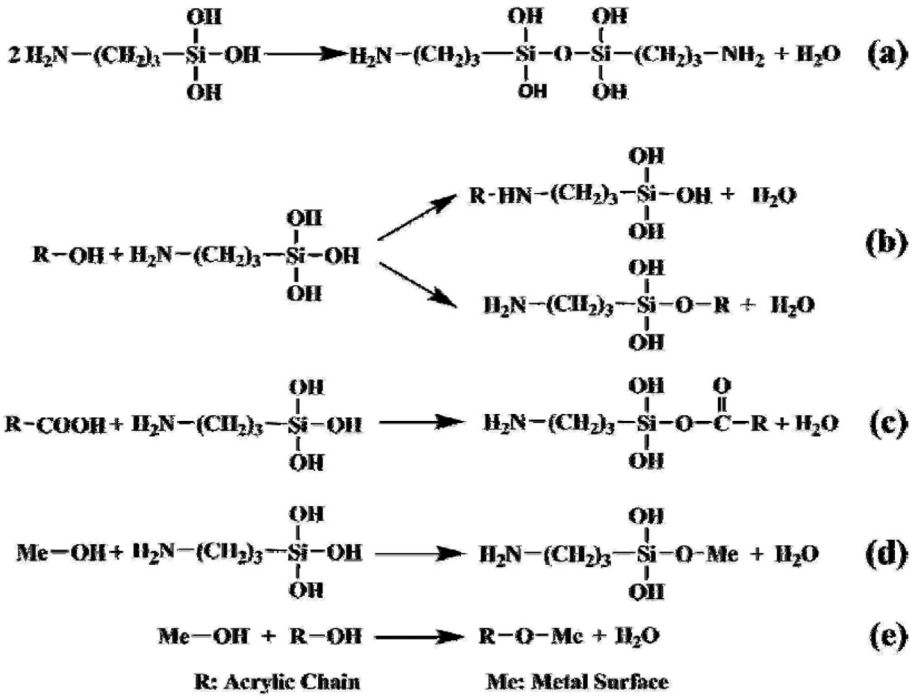

Scheme 2. The curing reaction mechanism of the curing process.

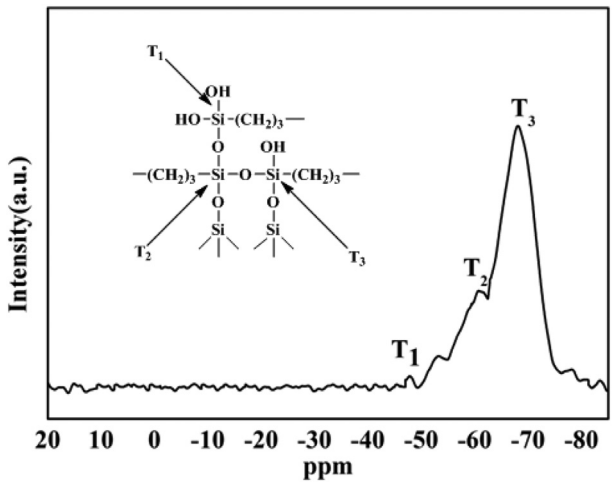

Fig. 2. The ^{29}Si NMR spectrum of WA/GMA15-KH-550 (1:0.15). The inset shows the dehydration reaction of KH-550 molecule.

Fig. 2. Three major peaks at about −66.79, −59.95 and −47.98 ppm were observed for the corresponding absorption of nonhydroxy-substituted silica (T_3), monohydroxy-substituted silica (T_2) and dihydroxy-substituted silica (T_1) [53], respectively. The relatively small peak integration area of the T_1 demonstrated the high conversion of the curing reaction of silanol groups and the formation of a silica network (Scheme 2a). Moreover, a small peak between T_1 and T_2 was observed at −53.73 ppm. This peak might arise from the absorption of the silicon center of the C-O-Si(R)(OH)O-Si- structure [54–57], which was formed through the dehydration reaction between the -COH groups of resins and the silanol group (Scheme 2b). From the ^{29}Si NMR results, the formation of the C-O-Si(R)(OH)-O-Si- structure also implied that the KH-550 was incorporated into the waterborne resin networks after curing.

In addition, the waterborne acrylic chain (R-OH) and KH-550 (Si-OH) can form hydrogen bonds with the hydroxyls (Me-OH) present on the metallic surface film. The remaining silanol groups that could not approach the metallic substrate form bonds among themselves. Upon curing or drying, these hydrogen bonds are converted to stable carbon-oxygen and siloxane bonds via the above reactions (Scheme 2a, 2d and 2e) [58–60]. The formative molecular layer through all the aforementioned reactions avoids the flash corrosion of the surface of the iron based material successfully.

The curing behavior of all samples was determined by non-isothermal DSC method. Figs. 3 and 4 show the typical DSC thermograms of waterborne resin samples in different conditions. These thermograms provide the information to determine the curing reaction condition. Fig. 3 shows the influence of the GMA amount on the curing temperature for WA/GMA-KH-550 (1:0.05) system. The initial temperature of curing reaction, peak temperature and finishing temperature are all decreased with increasing the GMA amount at a heating rate of 5 °C/min. Because the GMA is a class of functional material, part of epoxy functional groups will react with other polar functional groups that changes the structure of the acrylic branched chain in the process of synthesis, and can be easier crosslink with curing agent in the curing process. Meanwhile, the structure of the waterborne acrylic main chain modified with GMA has changed and a dense mesh structure is formed with the addition of curing agent. Therefore, the endothermic peak of curing reaction moves to a lower temperature (74.3 °C, 15 wt% GMA, 5 wt% KH-550), indicating an easier curing reaction. The WA/GMA-KH-550 (1:0), WA/GMA-KH-550 (1:0.15), and WA/GMA-KH-550 (1:0.3) all showed similar situations under the same curing conditions.

Fig. 4 shows the influence of the KH-550 amount on the curing for WA/GMA5-KH-550 system. The initial curing temperature is decreased after the incorporation of KH-550 at a heating rate of 5 °C/min. In other words, the waterborne resin filled with KH-550 has a much lower initiating curing temperature, indicating the effective curing of the KH-550 curing agent. Similarly, the peak curing temperature and finishing temperature are decreased after the incorporation of KH-550 compared to that of pure resin. The increased active site makes the curing process easier to form a three-dimensional network structure. Therefore, the endothermic peak of curing reaction moves to a lower temperature, and the curing reaction is accelerated. However, the 5 wt% KH-550 sample has the highest finishing temperature of 108.40 °C, which may be due to better dispersion of the KH-550 in system than other samples, and relatively high viscosity at last curing stage [61]. Thus, the rate of conversion is controlled by diffusion rather than kinetic factors in the last stage, thus the 5 wt% KH-550 sample will have the highest finishing temperature for the curing reaction. The KH-550 loading was observed to have a significant effect on the curing process. As compared to peak curing temperature of 92.83 °C for pure resin, the addition of 15 wt% KH-550 lowers the peak curing temperature to 79 °C. A higher KH-550 loading does not

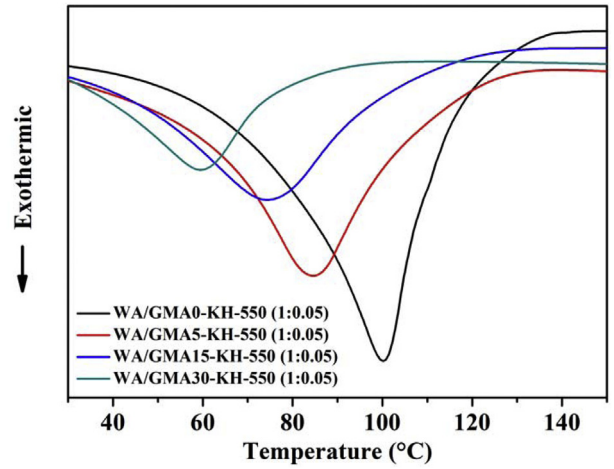

Fig. 3. Influence of the amount of GMA on curing of WA/GMA-KH-550 (1:0.05) system.

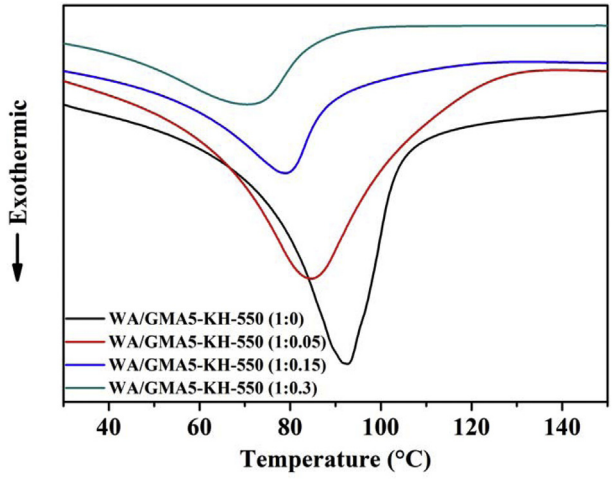

Fig. 4. Influence of the amount of KH-550 on the curing for WA/GMA5-KH-550 system.

significantly decrease the peak curing temperature. Thus, the best loading of the curing agent is 15 wt% KH-550. The WA/GMA0-KH-550, WA/GMA15-KH-550 and WA/GMA30-KH-550 showed all similar situations under the same curing conditions.

3.2. Thermal properties analysis

From the curing behavior, it can be concluded that the optimal loading of KH-550 is 15 wt%. The TGA curves of different GMA systems at the optimal loading of KH-550 were shown in Fig. 5. The residual rates of samples with different GMA contents are shown in Table 2. As seen from Fig. 5 and Table 2, the main weight loss took place at around 200–450 °C and the addition of GMA in the synthesis process could improve the heat resistance of materials. In addition, the residual weight of the resin modified with GMA also increased compared with pure acrylic coating from 100 to 400 °C. Because the boiling point of the KH-550 is 217 °C, and the small molecule KH-550 that does not participate in the curing reaction will rapidly lose at this temperature and form inflection points from 100 to 300 °C in different TGA curves. Meanwhile, the polar functional groups of different structures such as carboxyl and hydroxy that do not participate in the curing reaction will exhibit different degrees of condensation under different temperature and energy, forming small molecular water. The small molecule water will evaporate and causes the mass loss. When the residual weight of coatings is 85%, the coatings modified with 0 wt%, 5 wt%, 15 wt% and 30 wt% GMA corresponding temperature is 240.75 °C, 286.25 °C, 310.75 °C and 321.25 °C, respectively. When the residual weight of coatings is 80%, the coatings modified with 0 wt%, 5 wt%, 15 wt% and 30 wt% GMA corresponding temperature is 263 °C, 325.25 °C, 341.25 °C and 348.75 °C, respectively. All of these improvements indicated that the GMA was effective to enhance the thermal stability of the acrylic resin. The aforementioned results can be interpreted as two factors: first, because both the epoxy functional group and the hydroxyl group are able to react with the silicon hydroxyl groups to form much higher energy Si-O bond, as the content of GMA increases, the more Si-O is formed; second, the cross-linking density of the coatings also increases with the introduction of GMA, under this condition, the rotation, translation and moving of molecular chains and the escape of small molecules are hindered, which would form the three-dimensional network structure and it will need more energy to destroy the structure [18,61].

Table 2
The residual rates (wt%) of different GMA systems.

Temperature (°C)	0 wt%	5 wt%	15 wt%	30 wt%
150	93.89	95.76	97.98	98.95
200	90.55	94.59	95.83	96.79
250	82.74	88.84	91.44	92.77
300	75.00	83.43	86.27	87.48
350	66.03	75.62	77.87	79.70

3.3. Tensile properties analysis

Fig. 6 shows the typical tensile strain-stress curves of the cured coatings with different loadings of GMA. The tensile strength of the coatings is observed to depend on GMA amount. The tensile strength of cured pure acrylic resin is 7.26 MPa. The cured acrylic resin modified with 5 wt%, 15 wt% and 30 wt% GMA showed an enhanced tensile strength (8.79, 12.91 and 14.95 MPa) compared with that of cured pure acrylic resin. GMA can effectively increase the number of crosslink junctions between the waterborne resin and curing agent. Along with the increase of the GMA content, the junction increases and the final coating has a high cross-linking density, thus the tensile properties of the coating are increased. Moreover, the tensile strength of coating increases with the increase of GMA content, but its influence on the tensile strength is not very obvious when the GMA increases to a certain extent. The mechanism of the increased tensile strength is studied from the morphology of fracture surfaces (Fig. 7).

From the SEM morphologies (Fig. 7) of the fracture surface, the cured pure resin is observed to be very smooth and river-like (Fig. 7a), indicating that pure resin is very brittle, typical of thermosetting polymers [62]. The fracture surface becomes much rougher after modified with the GMA. The fracture surface of 30 wt % GMA (Fig. 7d) is much rougher and much wavier than others. A lot of voids are observed in the fracture surface of 15 wt% (Figs. 7c) and 30 wt% (Fig. 7d) GMA modified resin. Compared to unmodified resin, the resins modified with different loadings GMA showed better mechanical properties, which was possibly due to the increasing the crosslinking density of GMA modified resins and formed closed network structure [16,63,64]. In addition, the strong association of GMA with acrylic resin through covalent bonding also resulted in the increase of the mechanical properties of the acrylic resin.

There are some researches on the waterborne acrylic resin, the properties of other waterborne acrylic resin were compared.

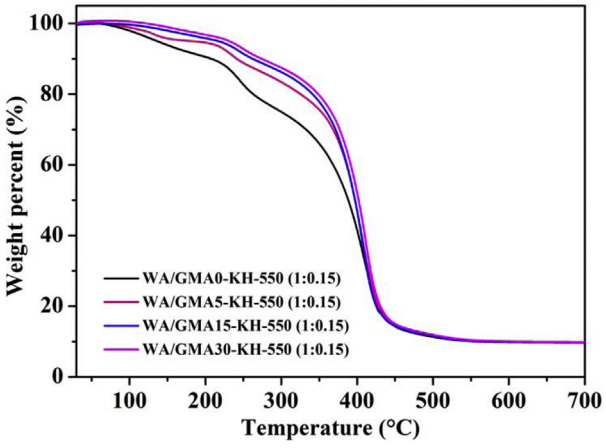

Fig. 5. TGA curves of different GMA systems.

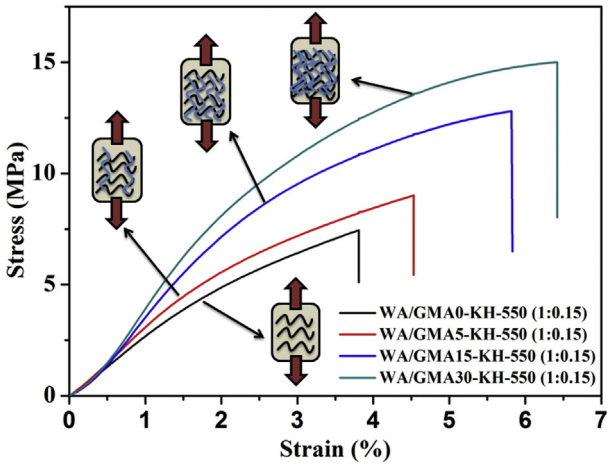

Fig. 6. Stress-strain curves of WA/GMA-KH-550 (1:0.15).

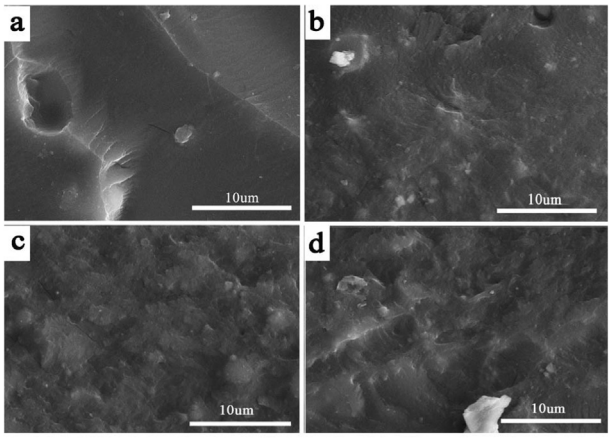

Fig. 7. SEM microstructures of the fracture surface of (a) WA/GMA0-KH-550 (1:0.15), (b) WA/GMA5-KH-550 (1:0.15), (c) WA/GMA15-KH-550 (1:0.15) and (d) WA/GMA30-KH-550 (1:0.15).

Table 3 lists the comparison of the resin type, curing temperature and tensile property of various waterborne acrylic resins. In this work, the novel waterborne acrylic resin modified with GMA not only has a relatively lower curing temperature, but also has a good tensile property.

3.4. Contact angle of the coatings

The surface wetting ability of coatings with various dosages of GMA and curing agent was evaluated by measuring the contact angle formed between the water drops and the surface of the samples using contact angle measuring system (Fig. 8). From Figure 8a, the contact angle increases with increasing of the GMA content in different KH-550 systems. It can be seen, that the contact angle of WA/GMA0-KH-550 (1:0.15) is 87.72°. However, after modification with GMA, it was found that WA/GMA15-KH-550 (1:0.15) showed an increase in contact angle up to 99.51°, indicating a hydrophobic nature of coating [65]. This demonstrates the modification effect on the surface wetting ability of the coating surface. From Figure 8b, the contact angle increases with the increasing of KH-550 amount. It could be that the KH-550 changed the physical and chemical properties of coating surface in the process of crosslink reaction [16,66]. In addition, the optimum amount of KH-550 is the same for different amounts of GMA. The contact angle of the WA/GMA15-KH-550 (1:0) was 85.56°. Upon adding 15 wt% KH-550, the formation of the coating was hydrophobic. It is noted that hydrophilicity depending on both surface roughness and the chemical crosslinking can lower surface energy sufficiently [67–70]. In present work, the low surface energy makes it a good candidate for the hydrophobic coating.

4. Conclusions

The waterborne coatings modified with GMA was prepared from various functional acrylic monomers by homogeneous solution polymerization in iso-propyl alcohol followed by solvent exchange with water. The curing temperature of the two-component waterborne resin was decreased obviously and the mechanical properties were also improved. At the same time, the KH-550 as the curing agent not only effectively increased the crosslinking density of the resin, but also combined with the tinplate to form the molecular layer of silicane. Thus, the addition of KH-550 effectively prevented the occurrence of flash corrosion. The as-prepared coatings with excellent mechanical, thermal and hydrophobic properties have potential applications in the areas of anti-flash corrosion, water purification, fire retardancy, chemical sensing, membrane, biomedical coating, waterproof and anti-corrosion

Table 3
Property comparison of several waterborne acrylic resins.

Type of resin	Curing temperature (°C)	Tensile strength (MPa)	Ref.
Acrylic	22.0	5.10	[19]
Acrylic-polyurethane	60.0	11.20	[69]
Acrylic-polyurethane	80.0	2.17	[70]
Acrylic-epoxy	50.0	7.52	[71]
Acrylic-KH-550	54.3	14.95	This work

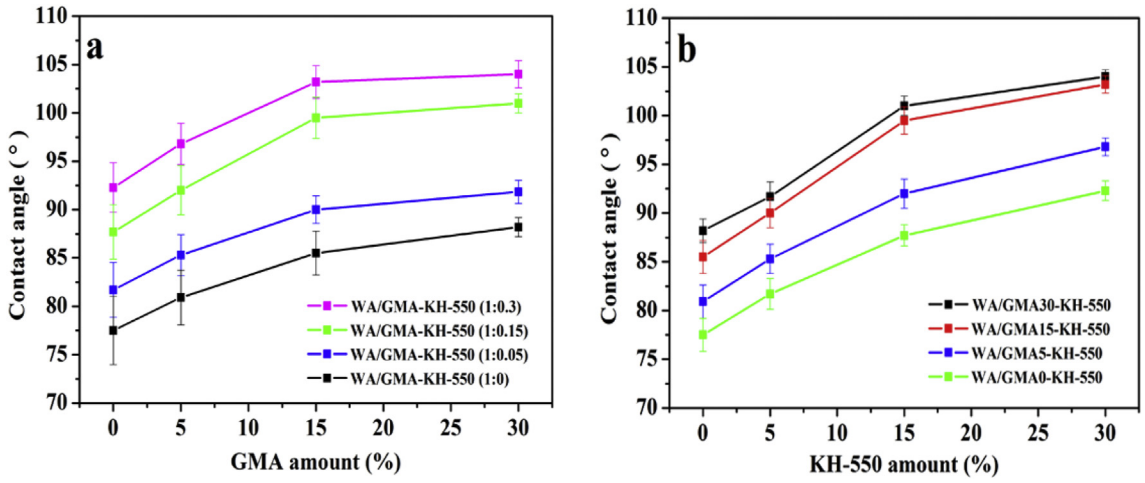

Fig. 8. (a) Influence of the GMA amount on the contact angle for different amount of KH-550. (b) Influence of the KH-550 amount on the contact angle for different amount of GMA.

coating [71–78]. With introducing functional nanofillers, the formed nanocomposites can have much broader applications such as structural materials [79–82], sensing [83–86], electromagnetic interference (EMI) shielding [87,88] and packaging materials [89].

References

[1] S. Huang, J. Xiao, Y. Zhu, Synthesis and properties of spray-applied high solid content two component polyurethane coatings based on polycaprolactone polyols, Prog. Org. Coating 106 (2017) 60–68.
[2] L. Zhang, M. Qin, W. Yu, Heterostructured TiO_2/WO_3 Nanocomposites for photocatalytic degradation of toluene under visible light, J. Electrochem. Soc. 164 (2017) H1086–H1090.
[3] S.A. Madbouly, Y. Xia, M.R. Kessler, Rheological behavior of environmentally friendly castor oil-based waterborne polyurethane dispersions, Macromolecules 46 (2013) 4606–4616.
[4] S. Awad, H. Chen, G. Chen, Free volumes, glass transitions, and cross-links in zinc oxide/waterborne polyurethane nanocomposites, Macromolecules 44 (2014) 29–38.
[5] M. Elrebii, A.B. Mabrouk, S. Boufi, Synthesis and properties of hybrid alkyd–acrylic dispersions and their use in VOC-free waterborne coatings, Prog. Org. Coating 77 (2014) 757–764.
[6] S. Saalah, L.C. Abdullah, M.M. Aung, Waterborne polyurethane dispersions synthesized from jatropha oil, Ind. Crop. Prod. 64 (2015) 194–200.
[7] J. Hu, J. Ma, W. Deng, Properties of acrylic resin/nano-SiO_2, leather finishing agent prepared via emulsifier-free emulsion polymerization, Mater. Lett. 62 (2008) 2931–2934.
[8] F. Chen, P. Liu, Conducting polyaniline nanoparticles and their dispersion for waterborne corrosion protection coatings, ACS Appl. Mater. Interfaces 3 (2011) 2694–2702.
[9] G. Wu, G. Liu, J. Chen, Preparation and properties of thermoset composite films from two-component waterborne polyurethane with low loading level nanofibrillated cellulose, Prog. Org. Coating 106 (2017) 170–176.
[10] D. Zhang, B.L. Williams, E.M. Becher, Flame retardant and hydrophobic cotton fabrics from intumescent coatings, Adv. Compos. Hybrid. Mater. 1 (2018) 177–184.
[11] J. Lin, X. Chen, C. Chen, Durably antibacterial and bacterially antiadhesive cotton fabrics coated by cationic fluorinated polymers, ACS Appl. Mater. Interfaces 10 (2018) 6124–6136.
[12] M.J. Monteiro, M.F. Cunningham, Polymer nanoparticles via living radical polymerization in aqueous dispersions: design and applications, Macromolecules 45 (2012) 4939–4957.
[13] P. Florian, K.K. Jena, S. Allauddin, Preparation and characterization of waterborne hyperbranched polyurethane-urea and their hybrid coatings, Ind. Eng. Chem. Res. 49 (2010) 4517–4527.
[14] S.K. Dhoke, A.S. Khanna, Electrochemical behavior of nano-iron oxide modified alkyd based waterborne coatings, Mater. Chem. Phys. 117 (2009) 550–556.
[15] J. Dai, S. Ma, Y. Wu, High bio-based content waterborne UV-curable coatings with excellent adhesion and flexibility, Prog. Org. Coating 87 (2015) 197–203.
[16] S. Paul, Water-borne acrylic emulsion paints, Prog. Org. Coating 5 (1977) 79–96.
[17] J. Li, L. Ecco, G. Delmas, In-situ AFM and EIS study of waterborne acrylic latex coatings for corrosion protection of carbon steel, J. Electrochem. Soc. 162 (2015) C55–C63.
[18] R. Dong, L. Liu, Preparation and properties of acrylic resin coating modified by functional graphene oxide, Appl. Surf. Sci. 2016 (368) (2016) 378–387.
[19] M.L. Picchio, M.C.G. Passeggi, M.J. Barandiaran, Waterborne acrylic–casein latexes as eco-friendly binders for coatings, Prog. Org. Coating 88 (2015) 8–16.
[20] X. Xu, H. Zhang, H. Lou, Chitosan-coated-magnetite with covalently grafted polystyrene based carbon nanocomposites for hexavalent chromium adsorption, Eng. Sci. (2018), https://doi.org/10.30919/espub.es.180308 (in press).
[21] L.G. Ecco, M. Fedel, F. Deflorian, Waterborne acrylic paint system based on nanoceria for corrosion protection of steel, Prog. Org. Coating 96 (2016) 19–25.
[22] S.M. Aqeel, Z. Huang, J. Walton, Polyvinylidene fluoride (PVDF)/polyacrylonitrile (PAN)/carbon nanotube nanocomposites for energy storage and conversion, Adv. Compos. Hybrid. Mater. 1 (2018) 185–192.
[23] Z. Lu, T. Tang, G. Zhou, Effects of dehumidification drying environment on drying speed of one component waterborne wood top coating, Appl. Surf. Sci. 365 (2016) 131–135.
[24] W. He, Y. Zhang, F. Luo, A novel non-releasing antibacterial poly (styrene-acrylate)/waterborne polyurethane composite containing gemini quaternary ammonium salt, RSC Adv. 5 (2015) 89763–89770.
[25] G. Yu, Y. Lu, J. Guo, Carbon nanotubes, graphene, and their derivatives for heavy metal removal, Adv. Compos. Hybrid. Mater. 1 (2018) 56–78.
[26] S.A. Madbouly, J.U. Otaigbe, Rheokinetics of thermal-induced gelation of waterborne polyurethane dispersions, Macromolecules 38 (2005) 10178–10184.
[27] S. Wang, W. Li, D. Han, Preparation and application of a waterborne acrylic copolymer-siloxane composite: improvement on the corrosion resistance of zinc-coated NdFeB magnets, RSC Adv. 5 (2015) 81759–81767.
[28] E.A. Papaj, D.J. Mills, S.S. Jamali, Effect of hardener variation on protective properties of polyurethane coating, Prog. Org. Coating 77 (2014) 2086–2090.
[29] C.A. Anagnostopoulos, Strength properties of an epoxy resin and cement-stabilized silty clay soil, Appl. Clay Sci. 114 (2015) 517–529.
[30] M. Melchiors, M. Sonntag, C. Kobusch, Recent developments in aqueous two-component polyurethane (2K-PUR) coatings, Prog. Org. Coating 40 (2000) 99–109.
[31] D.B. Otts, M.W. Urban, Heterogeneous crosslinking of waterborne two-component polyurethanes (WB 2K-PUR); stratification processes and the role of water, Polymer 46 (2005) 2699–2709.
[32] P.J.A. Geurink, T. Scherer, R. Buter, A complete new design for waterborne 2-pack PUR coatings with robust application properties, Prog. Org. Coating 55 (2006) 119–127.
[33] D.B. Otts, K.J. Pereira, W.L. Jarret, Dynamic colloidal processes in waterborne two-component polyurethanes and their effects on solution and film morphology, Polymer 46 (2005) 4776–4788.
[34] X. Xiang, F. Pan, Y. Li, A review on adsorption-enhanced photoreduction of carbon dioxide by nanocomposite materials, Adv. Compos. Hybrid. Mater. 1 (2018) 6–31.
[35] S. Wu, M.D. Soucek, Crosslinking of acrylic latex coatings with cycloaliphatic diepoxide, Polymer 41 (2000) 2017–2028.
[36] S. Gogoi, N. Karak, Biobased biodegradable waterborne hyperbranched polyurethane as an ecofriendly sustainable material, ACS Sustain. Chem. Eng. 2 (2014) 2730–2738.
[37] G. Wu, J. Chen, S. Huo, Thermoset nanocomposites from two-component waterborne polyurethanes and cellulose whiskers, Carbohydr. Polym. 105 (2014) 207–213.
[38] L. Chagnon, G. Arnold, S. Giljean, Elastic recovery and creep properties of waterborne two-component polyurethanes investigated by micro-indentation, Prog. Org. Coating 76 (2013) 1337–1345.
[39] Z. Ge, Y. Luo, Synthesis and characterization of siloxane-modified two-component waterborne polyurethane, Prog. Org. Coating 76 (2013) 1522–1526.
[40] H. Si, H. Liu, S. Shang, Preparation and properties of maleopimaric acid-based polyester polyol dispersion for two-component waterborne polyurethane coating, Prog. Org. Coating 90 (2016) 309–316.
[41] A. Kalendová, Methods for testing and evaluating the flash corrosion, Prog. Org. Coating. 44 (2002) 201–209.
[42] H.W. Engels, H.G. Pirkl, R. Albers, Polyurethanes: versatile materials and sustainable problem solvers for today's challenges, Angew. Chem. Int. Ed. 52 (2013) 9422–9441.
[43] C.E. Corcione, M. Frigione, Factors influencing photo curing kinetics of novel UV-cured siloxane-modified acrylic coatings: oxygen inhibition and composition, Thermochim. Acta 534 (2012) 21–27.
[44] F. Chen, P. Liu, Conducting polyaniline nanoparticles and their dispersion for waterborne corrosion protection coatings, ACS Appl. Mater. Interfaces 3 (2011) 2694–2702.
[45] X. Niu, L. Huo, C. Cai, Rod-like attapulgite modified by bifunctional acrylic resin as reinforcement for epoxy composites, Ind. Eng. Chem. Res. 53 (2014) 16359–16365.
[46] Y. Lin, J. Jin, M. Song, Curing dynamics and network formation of cyanate ester resin/polyhedral oligomeric silsesquioxane nanocomposites, Polymer 52 (2011) 1716–1724.
[47] R.V. Kulkarni, B.S. Mangond, S. Mutalik, Interpenetrating polymer network microcapsules of gellan gum and egg albumin entrapped with diltiazem–resin complex for controlled release application, Carbohydr. Polym. 83 (2011) 1001–1007.
[48] M. Nuopponen, T. Vuorinen, S. Jämsä, Thermal modifications in softwood studied by FT-IR and UV resonance Raman spectroscopies, J. Wood Chem. Technol. 24 (2005) 13–26.
[49] M.S. Shin, Y.H. Lee, M.M. Rahman, Synthesis and properties of waterborne fluorinated polyurethane-acrylate using a solvent-/emulsifier-free method, Polymer 54 (2013) 4873–4882.
[50] J. Hu, J. Ma, W. Deng, Properties of acrylic resin/nano-SiO2 leather finishing agent prepared via emulsifier-free emulsion polymerization, Mater. Lett. 62 (2008) 2931–2934.
[51] L. Zhang, H. Zhang, J. Guo, Synthesis and properties of UV-curable polyester-based waterborne polyurethane/functionalized silica composites and morphology of their nanostructured films, Ind. Eng. Chem. Res. 51 (2012) 8434–8441.
[52] S.K. Dhoke, R. Bhandari, A.S. Khanna, Effect of nano-ZnO addition on the silicone-modified alkyd-based waterborne coatings on its mechanical and heat-resistance properties, Prog. Org. Coating 64 (2009) 39–46.
[53] Y.L. Liu, C.S. Wu, Y.S. Chiu, Preparation, thermal properties, and flame retardance of epoxy-silica hybrid resins, Polym. Sci. Part A: Polym Chem. 41 (2003) 2354–2367.
[54] D.J. Lin, C.C. Chen, C.L. Chang, Observation of nano-particles in silica/poly (HEMA) hybrid by electron microscopy, J. Polym. Res. 9 (2002) 115–118.
[55] R.J.A. Hook, ^{29}Si NMR study of the sol-gel polymerisation rates of substituted ethoxysilanes, J. Non-Cryst. Solids 195 (1996) 1–15.
[56] Y.G. Hsu, I.L. Chiang, J.F. Lo, Properties of hybrid materials derived from hydroxyl-containing linear polyester and silica through sol-gel process. I. Effect of thermal treatment, J. Appl. Polym. Sci. 78 (2000) 1179–1190.
[57] Y.G. Hsu, K.H. Lin, Preparation and properties of ABS-silica nanocomposites

through sol-gel process under the catalyzation of different catalysts, J. Polym. Res. 8 (2001) 69–76.
[58] J. Liu, T. Xi, Enhanced anti-corrosion ability and biocompatibility of PLGA coatings on MgZnYNd alloy by BTSE-APTES pre-treatment for cardiovascular stent, J. Mater. Sci. Technol. 32 (2016) 845–857.
[59] I.G. De, J. Vereecken, A. Franquet, Silane coating of metal substrates: complementary use of electrochemical, optical and thermal analysis for the evaluation of film properties, Prog. Org. Coating 59 (2007) 224–229.
[60] A.M. Cabral, R.G. Duarte, M.F.A. Montemor, A comparative study on the corrosion resistance of AA2024-T3 substrates pre-treated with different silane solutions: composition of the films formed, Prog. Org. Coating 54 (2005) 322–331.
[61] J. Gao, H. Lv, X. Zhang, Synthesis and properties of waterborne epoxy acrylate nanocomposite coating modified by MAP-POSS, Prog. Org. Coating 76 (2013) 1477–1483.
[62] D. Jiang, Y. Huan, C. Sun, Thermal, mechanical and magnetic properties of functionalized magnetite/vinyl ester nanocomposites, RSC Adv. 6 (2016) 91584–91593.
[63] X. Zhang, V. Bitaraf, S. Wei, et al., Vinyl ester resin: rheological behaviors, curing kinetics, thermomechanical and tensile properties, AICHE J. 60 (2014) 266–274.
[64] S. Park, K.S. Lee, G. Bozoklu, Graphene oxide papers modified by divalent ions-enhancing mechanical properties via chemical cross-linking, ACS Nano 2 (2008) 572–578.
[65] M.H. Schneider, H. Willaime, Y. Tran, Wettability patterning by UV-initiated graft polymerization of poly (acrylic acid) in closed microfluidic systems of complex geometry, Anal. Chem. 82 (2010) 8848–8855.
[66] L. Zhai, M.C. Berg, F.C. Cebeci, Patterned superhydrophobic surfaces: toward a synthetic mimic of the namib desert beetle, Nano Lett. 6 (2006) 1213–1217.
[67] Q. Xie, J. Xu, L. Feng, Facile creation of a super-amphiphobic coating surface with bionic microstructure, Adv. Mater. 16 (2004) 302–305.
[68] X. Yang, L. Zhu, Y. Zhang, Surface properties and self-cleaning ability of the fluorinated acrylate coatings modified with dodecafluoroheptyl methacrylate through two adding ways, Appl. Surf. Sci. 295 (2014) 44–49.
[69] M.S. Shin, Y.H. Lee, M.M. Rahman, Synthesis and properties of waterborne fluorinated polyurethane-acrylate using a solvent-emulsifier-free method, Polymer 54 (2013) 4873–4882.
[70] H. Xu, F. Qiu, Y. Wang, Preparation, mechanical properties of waterborne polyurethane and crosslinked polyurethane-acrylate composite, J. Appl. Polym. Sci. 124 (2012) 958–968.
[71] G. Pan, L. Wu, Z. Zhang, Synthesis and characterization of epoxy-acrylate composite latex, J. Appl. Polym. Sci 83 (2002) 1736–1743.
[72] X. Cui, G. Zhu, Y. Pan, Polydimethylsiloxane-titania nanocomposite coating: fabrication and corrosion resistance, Polymer 138 (2018) 203–210.
[73] Y. Ma, L. Lyu, Y. Guo, Porous lignin based poly (acrylic acid)/organo-montmorillonite nanocomposites: swelling behaviors and rapid removal of Pb (II) ions, Polymer 128 (2017) 12–23.
[74] C. Wang, Y. Wu, Y. Li, et al., Flame-retardant rigid polyurethane foam with a phosphorus-nitrogen single intumescent flame retardant, Polym. Adv. Technol. 29 (2018) 668–676.
[75] L. Gao, L. Zhang, X. Lyu, Corrole functionalized iron oxide nanocomposites as enhanced peroxidase mimic and their application in H_2O_2 and glucose colorimetric sensing, Eng. Sci. (2018), https://doi.org/10.30919/espub.es.180314 (in press).
[76] C. Wang, B. Mo, Z. He, Hydroxide ions transportation in polynorbornene anion exchange membrane, Polymer 138 (2018) 363–368.
[77] C. Wang, Z. He, X. Xie, Controllable cross-linking anion exchange membranes with excellent mechanical and thermal properties, Macromol. Mater. Eng. (2018), https://doi.org/10.1002/mame.201700462 (in press).
[78] Z. Hu, D. Zhang, L. Yu, Y. Huang, Light-triggered C 60 release from a graphene/cyclodextrin nanoplatform for the protection of cytotoxicity induced by nitric oxide, J. Mater. Chem. B 6 (2018) 518–526.
[79] Z. Hu, Q. Shao, Y. Huang, Light triggered interfacial damage self-healing of poly (p-phenylene benzobisoxazole) fiber composites, Nanotechnology 29 (2018) 185602.
[80] K. Sun, R. Fan, X. Zhang, et al., An overview of metamaterials and their achievements in wireless power transfer, J. Mater. Chem. C 6 (2018) 2925–2943.
[81] Y. Guo, G. Xu, X. Yang, et al., Significantly enhanced and precisely modeled thermal conductivity in polyimide nanocomposites by chemically modified graphene via in-situ polymerization and electrospinning-hot press technology, J. Mater. Chem. C 6 (2018) 3004–3015.
[82] X. Wang, X. Liu, H. Yuan, et al., Non-covalently functionalized graphene strengthened poly (vinyl alcohol), Mater. Des. 139 (2018) 372–379.
[83] Y. Li, B. Zhou, G. Zheng, et al., Continuously prepared highly conductive and stretchable SWNT/MWNT synergistically composited electrospun thermoplastic polyurethane yarns for wearable sensing, J. Mater. Chem. C 6 (2018) 2258–2269.
[84] J. Zhao, L. Wu, C. Zhan, et al., Overview of polymer nanocomposites: computer simulation understanding of physical properties, Polymer 133 (2017) 272–287.
[85] H. Liu, W. Huang, X. Yang, et al., Organic vapor sensing behaviors of conductive thermoplastic polyurethane- graphene nanocomposites, J. Mater. Chem. C 4 (2016) 4459–4469.
[86] X. Guan, G. Zheng, K. Dai, et al., Carbon nanotubes-adsorbed electrospun PA66 nanofiber bundles with improved conductivity and robust flexibility, ACS Appl. Mater. Interfaces 8 (2016) 14150–14159.
[87] K. Zhang, G. Li, L. Feng, et al., Ultralow percolation threshold and enhanced electromagnetic interference shielding in poly(L-lactide)/multi-walled carbon nanotube nanocomposites with electrically conductive segregated networks, J. Mater. Chem. C 5 (2017) 9359–9369.
[88] J. Guo, H. Song, H. Liu, C. Luo, et al., Polypyrrole-interface-functionalized nano-magnetite epoxy nanocomposites as electromagnetic wave absorbers with enhanced flame retardancy, J. Mater. Chem. C 5 (2017) 5334–5344.
[89] Z. Wu, S. Gao, L. Chen, et al., Electrically insulated epoxy nanocomposites reinforced with synergistic core-shell SiO_2 @ MWCNTs and montmorillonite bifillers, Macromol. Chem. Phys. 218 (2017) 1700357.